Rare earth element diffusion in a natural pyrope single crystal at 2.8 GPa

Article *in* Contributions to Mineralogy and Petrology · August 2002

DOI: 10.1007/s004100100304

4 authors:

James A Van Orman
Case Western Reserve University
175 PUBLICATIONS **3,865** CITATIONS
SEE PROFILE

Timothy L Grove
Massachusetts Institute of Technology
420 PUBLICATIONS **22,875** CITATIONS
SEE PROFILE

Nobumichi Shimizu
Woods Hole Oceanographic Institution
133 PUBLICATIONS **7,973** CITATIONS
SEE PROFILE

Graham Layne
Memorial University of Newfoundland
136 PUBLICATIONS **5,012** CITATIONS
SEE PROFILE

Contrib Mineral Petrol (2002) 142: 416–424
DOI 10.1007/s004100100304

James A. Van Orman · Timothy L. Grove
Nobumichi Shimizu · Graham D. Layne

Rare earth element diffusion in a natural pyrope single crystal at 2.8 GPa

Received: 31 March 2001 / Accepted: 6 August 2001 / Published online: 8 September 2001

Abstract Volume diffusion rates of Ce, Sm, Dy, and Yb have been measured in a natural pyrope-rich garnet single crystal ($Py_{71}Alm_{16}Gr_{13}$) at a pressure of 2.8 GPa and temperatures of 1,200–1,450 °C. Pieces of a single gem-quality pyrope megacryst were polished, coated with a thin layer of polycrystalline REE oxide, then annealed in a piston cylinder device for times between 2.6 and 90 h. Diffusion profiles in the annealed samples were measured by SIMS depth profiling. The dependence of diffusion rates on temperature can be described by the following Arrhenius equations (diffusion coefficients in m^2/s):

$$\log_{10} D_{Yb} = (-7.73 \pm 0.97) - \left(343 \pm 30\,\mathrm{kJ\,mol^{-1}}/2.303RT\right)$$

$$\log_{10} D_{Dy} = (-9.04 \pm 0.97) - (302 \pm 30\,\mathrm{kJ\,mol^{-1}}/2.303RT)$$

$$\log_{10} D_{Sm} = (-9.21 \pm 0.97) - (300 \pm 30\,\mathrm{kJ\,mol^{-1}}/2.303RT)$$

$$\log_{10} D_{Ce}! = (-9.74 \pm 2.84) - (284 \pm 91\,\mathrm{kJ\,mol^{-1}}/2.303RT).$$

There is no significant influence of ionic radius on diffusion rates; at each temperature the diffusion coefficients for Ce, Sm, Dy, and Yb are indistinguishable from each other within the measurement uncertainty. However, comparison with other diffusion data suggests that there is a strong influence of ionic charge on diffusion rates in garnet, with REE^{3+} diffusion rates more than two orders of magnitude slower than divalent cation diffusion rates. This implies that the Sm–Nd isotopic chronometer may close at significantly higher temperatures than thermometers based on divalent cation exchange, such as the garnet–biotite thermometer. REE diffusion rates in pyrope are similar to Yb and Dy diffusion rates in diopside at temperatures near the solidus of garnet lherzolite (~1,450 °C at 2.8 GPa), and are an order of magnitude faster than Nd, Ce, and La in high-Ca pyroxene at these conditions. At lower temperatures relevant to the lithospheric mantle and crust, REE diffusion rates in garnet are much faster than in high-Ca pyroxene, and closure temperatures for Nd isotopes in slowly-cooled garnets are ~200 °C lower than in high-Ca pyroxene.

J.A. Van Orman (✉) · T.L. Grove
Department of Earth,
Atmospheric and Planetary Sciences,
Massachusetts Institute of Technology,
Cambridge, MA 02139, USA
E-mail: javanorm@alum.mit.edu

N. Shimizu · G.D. Layne
Department of Geology and Geophysics,
Woods Hole Oceanographic Institution,
Woods Hole, MA 02543, USA

Present address: J.A. Van Orman
Carnegie Institution of Washington,
Geophysical Laboratory and Department of
Terrestrial Magnetism,
5251 Broad Branch Rd.,
N.W., Washington, DC 20015, USA

Editorial responsibility: J. Hoefs

Introduction

Garnets are among the most useful recorders of the temperatures, pressures, and fluid interactions experienced by rocks from Earth's mantle and crust. Their utility stems from their involvement in chemical exchange reactions used for thermometry and barometry, from their use as isotopic chronometers (Sm–Nd, Lu–Hf), and from the chemical zoning profiles that they commonly preserve, which provide a record of growth conditions and subsequent diffusional modification. Interpreting the dynamic history of the host rock from the chemical and isotopic information stored in garnet crystals requires that diffusional transport rates be known under the appropriate conditions of temperature and pressure. Here we report the results of laboratory experiments designed to measure diffusion coefficients for Ce, Sm, Dy, and Yb in a natural pyrope crystal at a pressure of 2.8 GPa and temperatures between 1,200 and 1,450 °C. The pressure and temperature conditions of the experiments are within the regime of pyrope stability

(Boyd and England 1962), and thus we avoid difficulties that may be encountered in experiments at lower pressures where garnet is metastable. The conditions of the experiments are also within the range commonly experienced by upper mantle rocks (at temperatures approaching the garnet lherzolite solidus) making it unnecessary to extrapolate over a large P–T interval when modeling chemical and isotopic exchange in Earth's upper mantle. The rare earth elements chosen for study are important tracers of geochemical processes, and span a wide range of ionic radii (0.099 to 0.114 nm; Shannon 1976), making it possible to examine the influence of ionic radius on diffusion rates in garnet. Comparison with other experimental data sets allows us to evaluate the influence of ionic charge on diffusion as well.

Experimental methods

One section of a single pyrope megacryst was used for the diffusion experiments. The sample is from an ultramafic diatreme of the Colorado Plateau, and contained no visible cracks or inclusions. Another piece cut from the same crystal was used by Wang et al. (1996) in a study of hydrogen diffusion in pyrope, and the major and minor element composition of the crystal is given in that paper (their sample Py-6). The initial content of H_2O was 102 ± 10 ppm (Wang et al. 1996; FTIR measurement); no attempt was made to measure the hydrogen content after the REE diffusion anneals. The pyrope crystal was ground flat, in a random orientation, and polished to 0.06 μm alumina, then rinsed ultrasonically in a purified water bath. No further surface preparation was undertaken, and the sample was not pre-annealed because pyrope is not stable at atmospheric pressure.

A dilute nitric acid solution containing Ce, Sm, Dy, and Yb in equimolar proportions, with a total concentration of 750 ppm REE, was deposited onto the polished surface and then denitrified by heating at 800 °C for a few minutes. A thin layer of microcrystalline oxide particles remained on the surface, and this provided the tracer source for the diffusion experiments. After deposition of the tracer layer, the pyrope sample was cut into several pieces, each roughly cubical with an edge length of about 1 mm.

The diffusion anneals were performed in 12.7-mm diameter solid-medium piston-cylinder devices using techniques similar to those reported in Van Orman et al. (2001). A coated pyrope cube was loaded with graphite powder into a 4.45-mm diameter platinum outer capsule, taking care to position the coated surface in the center of the capsule. Four experiments were run with the pyrope cube in direct contact with the graphite powder. In two other experiments, the coated surface of the pyrope was placed against a polished disk of vitreous carbon (Alfa Aesar type II), and the pyrope/vitreous-carbon pair was separated from the graphite powder with two pieces of platinum foil. Each sample assembly was dried for 1 to 2 days at 120 °C, then the Pt outer capsule was welded shut, gently pounded flat, and placed within a high density alumina sleeve. The sample was centered within a graphite furnace using MgO spacers and then inserted into a $BaCO_3$ sleeve that served both as a thermal insulator and a soft pressure medium. Each run was pressed cold to 0.7 GPa, then heated to 865 °C at 50 °C/min. After holding at these conditions for 6 min, the sample was compressed to 2.8 GPa while heating to the final run temperature at a rate of 100 °C/min. The samples were held at constant temperature and pressure for times between 2.6 and 90 h, then quenched by shutting off the power. After quenching, the pyrope cube was carefully extracted from the Pt capsule and rinsed in ethanol to remove any graphite clinging to the surface. Pyrope cubes that were placed in direct contact with graphite powder could be extracted as whole pieces, whereas samples that were placed in contact with the vitreous carbon disk parted along several planes parallel to the pyrope/glassy-carbon interface. In every case, however, the coated surface of the pyrope crystal was recovered intact.

Temperature was monitored during each experiment with a $W_{97}Re_3$–$W_{75}Re_{25}$ thermocouple that was separated from the Pt capsule by a thin crushable MgO wafer. The temperature difference between the center of the capsule and the position of the thermocouple has been determined to be ~20 °C using offset thermocouples, and temperatures reported in Table 1 are corrected for this difference. No correction for the effect of pressure on thermocouple emf has been applied. The oxygen fugacity in each experiment, if buffered by the equilibrium between graphite and C–O fluid (Ulmer and Luth 1991; Frost and Wood 1995), was in the range $10^{-7.7}$ (at 1,200 °C) to $10^{-5.9}$ (at 1,450 °C).

Pyrope crystals that were annealed in contact with graphite powder bore the imprint of the polycrystalline

Table 1 Summary of run conditions and diffusion data for Ce, Sm, Dy, and Yb in pyrope at 2.8 GPa

Run	Capsule Configuration	T[a] (°C)	Duration (h)	D_{Ce} ($\times 10^{21}$ m^2/s)	D_{Sm} ($\times 10^{21}$ m^2/s)	D_{Dy} ($\times 10^{21}$ m^2/s)	D_{Yb} ($\times 10^{21}$ m^2/s)
C229	Graphite	1,450	4.0	405 ± 122	360 ± 106	484 ± 141	492 ± 145
B619	Graphite	1,400	24.0	352 ± 152	304 ± 132	484 ± 210	484 ± 210
B738	Vitreous C	1,400	2.6	–	324 ± 96	453 ± 134	596 ± 169
D30	Graphite	1,350	20.2	155 ± 45	169 ± 49	144 ± 43	139 ± 42
C223	Graphite	1,300	90.0	–	94 ± 57	103 ± 55	125 ± 83
B740	Vitreous C	1,200	40.3	–	12.7 ± 3.8	17.4 ± 5.2	12.0 ± 3.5

[a] Temperature uncertainties are estimated to be ±10 °C

confining medium on their coated surfaces. The pyrope surface was visibly roughened after the experiment, and surface profilometer scans showed that the mean surface roughness had increased from 5–10 nm in coated, unannealed samples to 30–50 nm after the anneal. Samples that were annealed in contact with the vitreous carbon disk maintained a mirror finish on their coated surfaces, with no increase in surface roughness after the experiment.

The samples were mounted in epoxy with the tracer-coated surface exposed and covered with a thin (~20-nm) gold film in preparation for SIMS depth profiling analysis. Most of the analyses were performed using the Cameca IMS 3f ion microprobe at the Woods Hole Oceanographic Institution, using the same general procedure discussed in Van Orman et al. (2001). A 10-nA O^- primary beam was rastered over a square area 50 μm on a side, and sampling was restricted to a circle 8 μm in diameter through the use of a mechanical field aperture carefully centered over the sputtered area. ^{30}Si, ^{44}Ca, ^{140}Ce, ^{147}Sm, and/or ^{152}Sm, ^{164}Dy, and ^{174}Yb intensities were monitored, with the secondary voltage offset by –50 V to reduce molecular interferences. The gold coat was removed after the analysis by ultrasonically rinsing the sample in a potassium iodide solution, and the depths of the sputtered pits were measured using a Dektak 8000 diamond-tipped stylus profilometer.

The solubility of Ce in pyrope is very low and, because of its low concentration in the annealed samples, profiles of ^{140}Ce could not be detected reliably using the IMS 3f ion microprobe. Three of the samples were therefore re-analyzed with the IMS 1270 ion microprobe at the Woods Hole Oceanographic Institution, which has significantly lower detection limits. The diffusion data for Ce reported in Table 1 were all obtained from depth profiles using the IMS 1270, and all other data are from IMS 3f profiles.

Diffusion coefficients were determined by fitting the REE concentration profiles to an error function solution to the diffusion equation. The pyrope crystal was considered to represent a semi-infinite medium, and the concentration at the interface between the pyrope and REE oxide layer was assumed to have been constant throughout the experiment. The solution to the diffusion equation in this case is:

$$\frac{C(x,t) - C_0}{C_i - C_0} = erf\left(\frac{x}{2\sqrt{Dt}}\right), \quad (1)$$

where C refers to the concentration at depth x after annealing time t, C_0 is the concentration at the interface, C_i is the initial concentration in the pyrope crystal, and D is the diffusion coefficient. Experiments run at the same pressure and temperature conditions for different times had similar concentrations of REE near the surface of the crystal, indicating that the constant concentration boundary condition was satisfied. Although diffusion took place in a REE concentration gradient, and therefore a gradient in chemical potential, REE are probably present at sufficient dilution that the measured diffusion coefficients are similar to self-diffusion coefficients. There is no evidence from the shapes of the diffusion profiles that diffusion rates depend significantly on REE concentration. Diffusion coefficients were evaluated by plotting the inverse error function of the left-hand side of Eq. (1) versus depth. This results in a straight line of slope $(4Dt)^{-1/2}$ provided that the data satisfy the conditions of the diffusion model. The erf^{-1} profiles were fit by linear least squares regression, with the value of C_0 adjusted by an iterative procedure until the fitted line passed through the origin. Representative diffusion profiles from a sample annealed in contact with graphite powder at 1,450 °C are shown in Fig. 1.

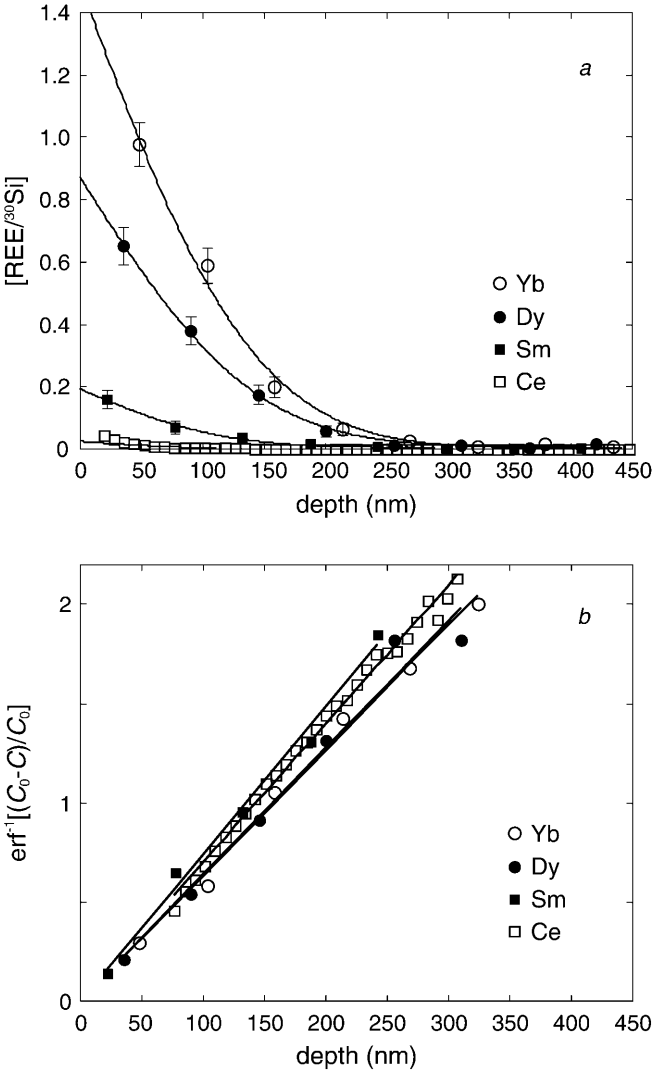

Fig. 1 **a** Typical diffusion profiles **b** and their error function inversions. Experiment C229:1,450 °C, 4 h. The *error bars* in **a** reflect the 1σ statistical uncertainty in [REE/^{30}Si] values and are dominated by the uncertainty in the REE counts, which were estimated assuming Poisson statistics (i.e., $\sigma = \sqrt{N}$ where N is the number of counts). The relative uncertainty decreases with the number of counts as $\sqrt{N}/N$

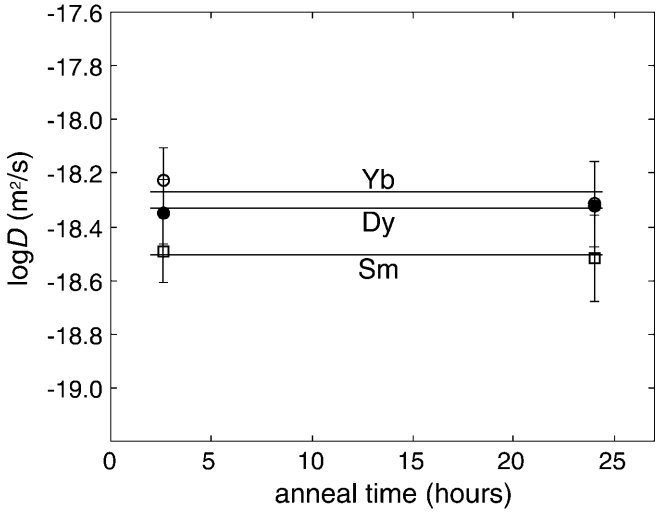

Fig. 2 Time series at 1,400 °C. Diffusion coefficients for Yb, Dy, and Sm are independent of the anneal duration, consistent with transport by volume diffusion

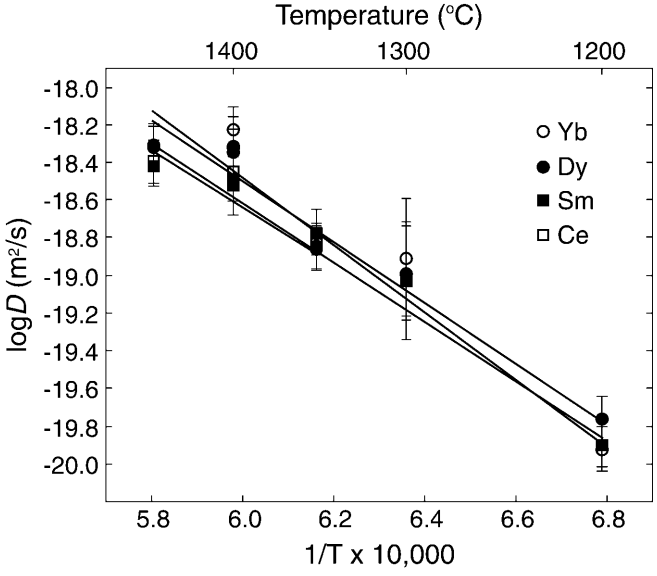

Fig. 3 Arrhenius plot showing Yb, Dy, Sm, and Ce diffusion coefficients from this study versus T^{-1}. Values of D_0 and H determined from linear regression of each data set are given in Table 2

Results

The results of the diffusion experiments are listed in Table 1. The reported uncertainties in D values (1σ) were estimated by considering the error in SIMS crater depth measurements (typically 5–10%) and the statistical uncertainty in fitting the profiles to equation 1 (which was small in comparison). Two experiments performed at 1,400 °C for times of 2.6 and 24 h yielded similar diffusion coefficients (Fig. 2). The close agreement between these experiments shows that the diffusion coefficients are independent of time, and indicates that transport of REE into the pyrope crystal was indeed accomplished by volume diffusion. No difference in diffusivity was observed between experiments in which the garnet crystal was in contact with graphite powder and experiments in which the sample was in contact with a vitreous carbon disk (Table 1). The greater surface roughness of the samples annealed in graphite powder resulted in somewhat poorer depth resolution in the SIMS depth profiling analysis, but this introduced no significant bias in estimating the diffusion coefficients.

Diffusion coefficients for each element are plotted as a function of inverse temperature in Fig. 3. The data for each element define a linear trend on the plot and are consistent with an Arrhenius relationship, $D = D_0 e^{-H/RT}$. Values of the pre-exponential factor D_0 and activation enthalpy H ($\equiv E + PV$) obtained by linear least-squares regression of the diffusion data are listed in Table 2. The uncertainties (reported as 1σ in Table 2) in H and D_0 were estimated from the linear regression, taking into account the estimated error in D and $1/T$ for each data point. Temperature is believed to be reproducible in our piston cylinder sample assemblies to within ±10 °C. No attempt was made to include the uncertainty in the pressure measurements, but this is believed to be only

Table 2 Arrhenius parameters ($D = D_0 e^{-H/RT}$) for diffusion in pyrope at 2.8 GPa

Element	$Log_{10}D_0$ (m^2/s)	H (kJ/mol)
Yb	–7.73 ± 0.97	343 ± 30
Dy	–9.04 ± 0.97	302 ± 30
Sm	–9.21 ± 0.97	300 ± 30
Ce	–9.74 ± 2.84	284 ± 91

~0.05 GPa and does not lead to a significant error in D for reasonable estimates of the activation volume.

At each temperature, the diffusion coefficients for Ce, Sm, Dy, and Yb are indistinguishable from each other within the measurement uncertainty (Table 1). This is in striking contrast to the behavior of REE in diopside (Van Orman et al. 2001) and zircon (Cherniak et al. 1997) where diffusion rates are found to decrease smoothly with increasing ionic radius. As discussed below, the insensitivity of diffusion rates to ionic radius appears to apply quite generally to both aluminosilicate and aluminate garnets, at least for cations that partition onto the 8-fold site.

Discussion

Figure 4 shows an Arrhenius plot comparing our data with other rare earth element diffusion data in aluminosilicate and aluminate garnets. The diffusion coefficients determined by Harrison and Wood (1980) for samarium in pure pyrope are more than two orders of magnitude higher than our data, under similar pressure and temperature conditions. The Harrison and Wood

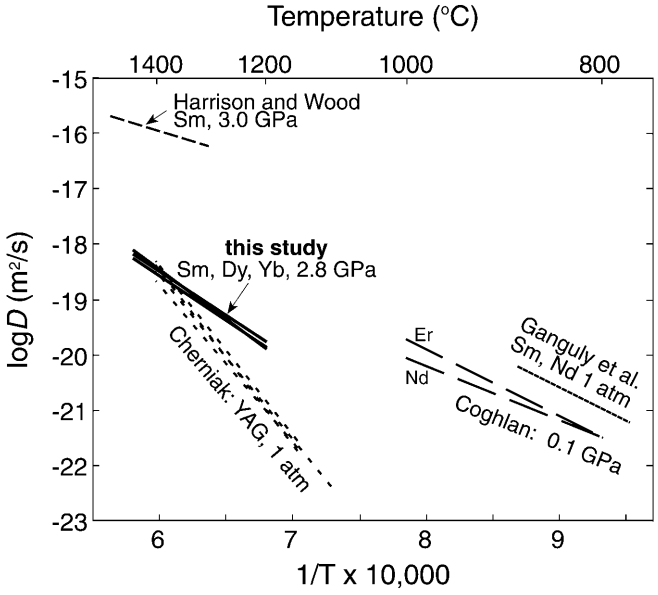

Fig. 4 Comparison of diffusion data obtained in this study with other published data for rare earth elements in aluminosilicate and aluminate garnets. References: Harrison and Wood (1980); Coghlan (1990); Cherniak (1998); Ganguly et al. (1998)

(1980) data were estimated from the time required to attain steady state partitioning between ~10 micron pyrope crystals and a silicate melt (at 3.0 GPa). The high apparent diffusivities and low activation energies that they obtained suggest that a process other than volume diffusion in the garnet may have been responsible for Sm transfer between garnet crystals and melt in their experiments. Coghlan (1990) determined Nd and Er diffusion coefficients in metastable almandine ($Alm_{67}Sp_{28}An_3Py_2$) single crystals from hydrothermal experiments at 0.1 GPa and 800–1,000 °C, using an isotopically enriched aqueous tracer solution as the diffusion source. Coghlan's data, extrapolated to the temperatures of our experiments, are in reasonable agreement with our data, despite major differences in garnet composition, pressure and hydrogen fugacity between the two sets of experiments.

Ganguly et al. (1998) measured Sm and Nd diffusion coefficients in metastable almandine ($Alm_{75}Py_{22}$) single crystals at 1 bar and 777–877 °C, using thin film and ion probe depth profiling techniques similar to those we have employed. The extension of their Arrhenius trend, uncorrected for pressure, plots more than an order of magnitude above our data. Although no experimental estimate of the activation volume for REE diffusion in garnet is available, the activation volume for Mg tracer diffusion is ~8 cm^3/mol (Chakraborty and Rubie 1996) and for Ca–(Mg, Fe) inter-diffusion is11.2 cm^3/mol (Freer and Edwards 1999). If the activation volume for rare earth element diffusion is similar (~10 cm^3/mol), then the Arrhenius curve of Ganguly et al. (1998), corrected to 2.8 GPa, lies about one order of magnitude above our data. This discrepancy may arise from the error involved in extrapolating the data over a large temperature (and pressure) interval, or may indicate a dependence of REE diffusion rates on the composition of the garnet. Chakraborty and Rubie (1996) reported a small yet significant increase in Mg tracer diffusion rates with increasing almandine content, and if this trend also applies to REE diffusion it may account for the difference between our measurements and those of Ganguly et al. (1998). The activation enthalpy of 254 kJ/mol calculated by Ganguly et al. (1998) for Nd and Sm diffusion at 1 bar is similar to the activation enthalpies we have obtained, and even more so if the effect of pressure is considered. Corrected to 1 bar using an activation volume of 10 cm^3/mol, our activation enthalpies are in the range 256–315 kJ/mol.

Also shown in Fig. 4 are diffusion data for La, Nd, Dy, and Yb in yttrium aluminum garnet (YAG) determined by Cherniak (1998). The data for REE diffusion in YAG are similar to our data at temperatures of 1,300–1,400 °C but the activation enthalpies for YAG are much higher (~540–600 kJ/mol), and diffusion rates in YAG at lower temperatures are significantly slower than in aluminosilicate garnets.

None of the studies of rare earth element diffusion in garnet show any significant influence of ionic radius on diffusion rates. This is surprising, because according to the elastic strain model presented by Van Orman et al. (2001) a significant dependence of D on ionic radius is expected. The similarity in eightfold site size (Smyth and Bish 1988; Blundy and Wood 1994; Van Westrenen et al. 1999) and elastic moduli and their temperature derivatives (Bass 1995) in high-Ca pyroxene and garnet would lead one to expect that the D-ionic radius relationship would be broadly similar in the two minerals. Aluminosilicate garnets also have lower activation enthalpies for diffusion than would be expected based on their relatively large elastic moduli. Cherniak (1998) showed that activation enthalpies for REE diffusion in calcite, apatite, diopside, titanite, YIG and YAG garnets, zircon, and corundum display a fairly tight linear relationship with bulk modulus, but that activation enthalpies for aluminosilicate garnet (from Coghlan 1990) fall well below this trend. Our activation enthalpies are similar to those found by Coghlan (1990), and fall well below the trend defined by the other minerals.

Because it is not possible to positively identify the diffusion mechanism in our experiments, we can only speculate on why REE diffusion coefficients in pyrope are insensitive to ionic radius. One possibility is that REE diffusion is limited by the coupled transport of another ion, but for several reasons this seems unlikely. The rare earth elements are probably incorporated via exchange with Mg (and other divalent cations that occupy the eight-fold site), with the excess charge likely balanced by the formation of vacancies on one or more cation sites. In this case it is expected that REE limit the rate of transport, because divalent cation and vacancy diffusion rates are significantly faster than those we have measured for the REE (Chakraborty and Ganguly 1992; Chakraborty and Rubie 1996; Freer and Edwards 1999).

If, on the other hand, REE–Al exchange were responsible for REE incorporation, then Al might limit the rate of exchange. However, direct REE-Al exchange seems unlikely. There is no evidence from partitioning experiments that – at concentration levels similar to or lower than in our experiments – REE can occupy the octahedral Al site (e.g., Van Westrenen et al. 1999). Coupled exchange also does not appear to explain the lack of a *D*-ionic radius dependence for the REE in yttrium aluminum garnet (Cherniak 1998), where REE exchange directly with an ion (Y^{3+}) of the same charge and intermediate ionic radius. The same is true of divalent cation diffusion in aluminosilicate garnets, where Ca, Fe, Mn, and Mg are found to diffuse at very similar rates (Chakraborty and Ganguly 1992; Freer and Edwards 1999). A likely explanation for the insensitivity of diffusion rates to ionic radius in aluminosilicate and aluminate garnets is that little elastic strain energy is dissipated when a cation moves from one site to another. Why this appears to be so for garnets, but not for other minerals such as clinopyroxene (Van Orman et al. 2001), zircon (Cherniak et al. 1997), plagioclase (Giletti and Shanahan 1997; LaTourrette and Wasserburg 1998), and periclase (e.g., Wuensch 1982), is not clear.

Although there is no significant dependence of diffusion rates on ionic radius, diffusion rates in garnet do appear to decrease significantly with increasing ionic charge. Figure 5 compares our data for rare earth element diffusion in pyrope with two different data sets for divalent cation diffusion collected under similar P–T conditions (Chakraborty and Ganguly 1992; Freer and Edwards 1999). Divalent cation diffusion rates in garnet are more than two orders of magnitude faster than trivalent REE diffusion rates at the same pressure and temperature. This large difference in diffusivity between REE and divalent cations has important implications for the interpretation of thermal histories of metamorphic rocks. It indicates that the Sm–Nd isotopic system in garnet is considerably more resistant to diffusional resetting than major element cation exchanges used for thermometry, such as the garnet–biotite Fe–Mg exchange thermometer. Although there are no experimental diffusion data for divalent cations in biotite, diffusion rates of other ions are many orders of magnitude faster in biotite than in garnet (Brady 1995), and thus garnet is expected to limit the bulk rate of exchange. This implies that, in slowly cooled rocks, the garnet–biotite exchange thermometer should lock in long after the Sm–Nd isotopic chronometer.

In Fig. 6 rare earth element diffusion rates in pyrope are compared with REE diffusion rates in diopside. At temperatures of 1,300–1,400 °C, REE diffusion rates in pyrope are similar to Yb and Dy diffusion rates in diopside, and are about an order of magnitude faster than Nd, Ce, and La in diopside. At lower temperatures the Arrhenius curves diverge. Rare earth element diffusion rates in pyrope, extrapolated to 900 °C, are more than an order of magnitude faster than Yb and three orders of magnitude faster than Nd in diopside. As a consequence of the lower activation enthalpy for diffusion in garnet, REE closure temperatures in garnet are significantly lower than in diopside (Fig. 7). For spherical crystals 1 mm in diameter cooling at 1 to 100 °C million years^{-1}, the closure temperature for Nd in

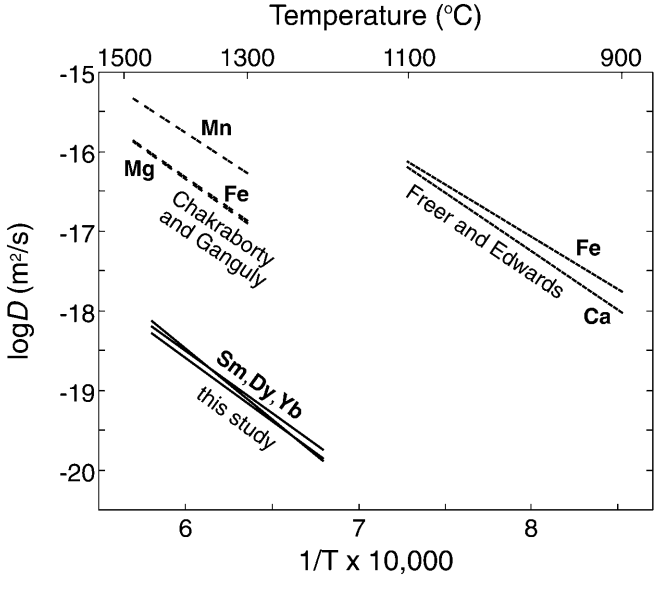

Fig. 5 Arrhenius plot comparing REE diffusion data obtained in this study with diffusion data for divalent cations obtained under similar conditions. All data are corrected to 2.8 GPa using activation volumes given in the data sources (Chakraborty and Ganguly 1992; Freer and Edwards 1999)

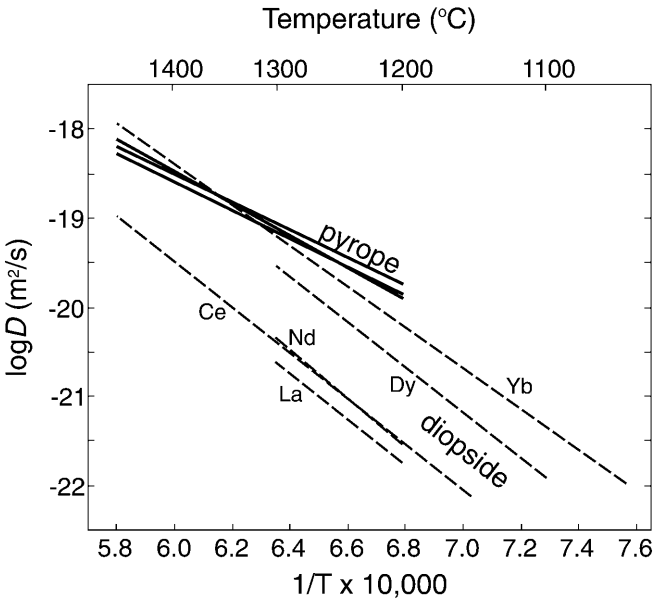

Fig. 6 Comparison of REE diffusion rates in pyrope (this paper; *solid lines*) and diopside (Van Orman et al. 2001). The diopside data are corrected to 2.8 GPa using the activation volume (~9 cm^3/mol) reported in that paper

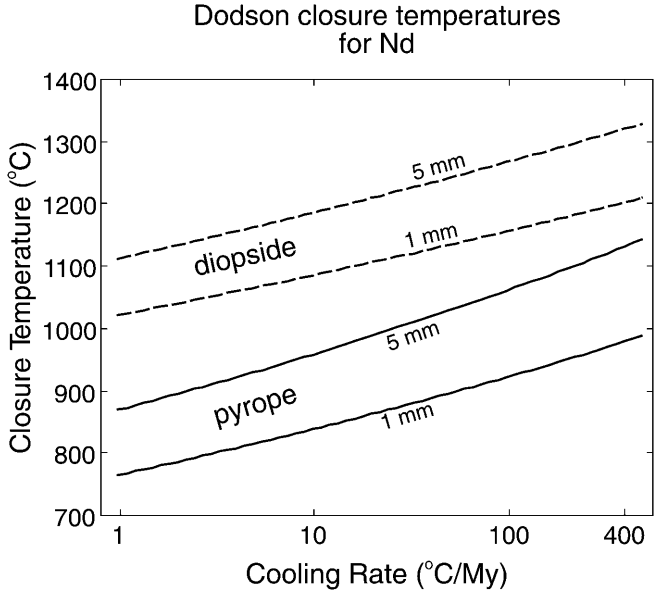

Fig. 7 Closure temperatures for Nd in pyrope and diopside spheres at 1 GPa, calculated using the Dodson formulation (Dodson 1973). Activation volumes of 10 and 9 cm^3/mol were used to calculate the 1-GPa activation enthalpies for pyrope and diopside, respectively. For a given grain size and cooling rate, the Dodson equation is valid only if the initial temperature is high enough for diffusion to significantly affect the core composition (Ganguly and Tirone 1999). For 1-mm pyrope spheres, the peak temperature must be at least 910 °C for a cooling rate of 1 °C/million years, and at least 1,180 °C for a cooling rate of 400 °C/million years. For 1 mm diopside, peak temperatures must be 1,150 and 1,360 °C for cooling rates of 1 and 400 °C/million years, respectively. If peak metamorphic temperatures are lower than these values, then the Dodson equation overestimates the closure temperature, and the extended solution of Ganguly and Tirone (1999) must be used. *Dashed lines* – diopside; *solid lines* – pyrope. *Numbers on curves* indicate the grain diameter in millimeters

pyrope is in the range 765–920 °C, and for diopside is about 200 °C higher. These closure temperatures are calculated from the Dodson equation (Dodson 1973), which holds only if the extent of diffusion is sufficient to significantly affect the composition at the core of a solid grain (Ganguly and Tirone 1999). If the initial temperature at which the mineral equilibrated is lower than a certain threshold value (which varies with the grain size and cooling rate), then the Dodson equation will overestimate the true closure temperature (Ganguly and Tirone 1999). The Dodson closure temperatures for Nd in garnet that we have estimated from our experimental data are similar to the empirical closure temperature estimate of Jagoutz (1988) for slowly cooled eclogite xenoliths from Tanzania (~850 °C), but higher than the estimate of Mezger et al. (1992) for granulites and amphibolites from the Superior Province and Grenville orogen (~600 °C). The discrepancy in closure temperature estimates may be, in part, caused by the lower peak temperatures of the rocks studied by Mezger et al. (1992). The peak temperature experienced by the Pikwitonei granulite is estimated to be ~750 °C (Mezger et al. 1992), and considering the grain size of 1–5 mm and inferred cooling rate of a few degrees per million years, this initial temperature is too low for the Dodson equation to apply. The extended formulation of Ganguly and Tirone (1999) must be used instead, and this gives a closure temperature of ~730 °C for the Pikwitonei rocks (with diffusion coefficients corrected for pressure assuming a 10 cm^3/mol activation volume). This is still higher than the empirical estimate, but the agreement improves if the initial cooling rate of the rocks is slower than inferred by Mezger et al. (1992), or if activation energies at the lower end of our experimental uncertainty envelope are used.

The experimental data presented in this paper and in Van Orman et al. (2001) indicate that at temperatures below ~1,400 °C, clinopyroxene will limit the diffusive mass transfer of REE in rocks that contain both garnet and clinopyroxene. This is consistent with geochemical observations in granulites from the Bergen Arcs in western Norway (Burton et al. 1995), where garnet adjacent to clinopyroxene preserves significantly older Sm/Nd ages than garnet adjacent to any other mineral. It is also consistent with major element zoning profiles preserved in eclogite xenoliths from the Roberts Victor kimberlite (Sautter and Harte 1990), in which exsolved garnet lamellae preserve compositional gradients that are far more extensively relaxed than in adjacent clinopyroxene. In contrast, observations in some peridotite xenoliths appear to suggest that clinopyroxene equilibrates more rapidly than co-existing garnet. While major and trace element zoning in garnet crystals within peridotite xenoliths is common, chemical zoning is usually absent in high-Ca pyroxene crystals from the same rocks (e.g., Griffin et al. 1989; Smith et al. 1991; Smith and Boyd 1992). There are at least two interpretations of this observation that are consistent with the experimental garnet and clinopyroxene diffusion data. One is that diffusion profiles actually do exist in the clinopyroxene, but that their length is too short to be detected by microbeam methods. A second possibility is that clinopyroxene crystals in these rocks are not primary, but have precipitated from or recrystallized in the presence of a silicate melt or fluid (e.g., Shimizu 1999). Peridotite samples in which garnet zoning has been observed in the absence of any detectable chemical zoning in co-existing pyroxene commonly preserve clear evidence for interaction with metasomatic fluids. Clinopyroxene might interact with infiltrating fluids via a dissolution/precipitation process, whereas reaction between garnet and fluid is controlled by diffusion. In any case, the body of experimental data on cation diffusion in clinopyroxene and garnet indicates that clinopyroxene has the more sluggish diffusion kinetics at temperatures below ~1,400 °C, and this experimental constraint provides an important bound on the interpretation of data from natural samples. A further potential constraint on the nature of zoning profiles in garnet arises from the large difference in diffusion rates of 2+ and 3+ ions. Some garnets from cratonic peridotites in South Africa and

Siberia (Shimizu 1999; Shimizu et al. 1999) preserve zoning profiles for Sr (2+), Y (3+), and Zr (4+) that are similar to each other in wavelength and in form. These profiles must be essentially unmodified growth features because any significant diffusion would have led to 2+ profiles that were far more relaxed than 3+ (or presumably 4+) profiles.

Conclusions

We have reported the results of isothermal annealing experiments designed to measure volume diffusion rates of Ce, Sm, Dy, and Yb in a natural pyrope single crystal at high pressure. Despite significant differences in ionic radius among these elements (0.114 to 0.099 nm; Shannon 1976) there is no perceptible difference in diffusion rates. There are significant differences between diffusion rates of trivalent and divalent cations in aluminosilicate garnets, however. At similar pressures and temperatures, Ca, Fe, Mg, and Mn diffusion rates (Chakraborty and Ganguly 1992; Freer and Edwards 1999) are more than two orders of magnitude faster than the REE diffusion rates we report. Closure of divalent cation exchange thermometers, if controlled by diffusion in garnet, will thus occur at significantly lower temperatures than closure of the Sm–Nd isotopic system. At temperatures below ~1,500 °C, Nd diffusion rates in pyrope are more rapid than in high-Ca pyroxene (Van Orman et al. 2001), and thus under most conditions high-Ca pyroxene is expected to control the exchange of Nd isotopes in rocks that contain both minerals.

Acknowledgements We thank Liping Wang for providing the pyrope crystal used in this study, and gratefully acknowledge helpful discussions with Ben Harte and constructive reviews by John Brady and an anonymous reviewer. This work was supported by grants from the National Science Foundation (OCE-9415968 and OCE-9731506) and by an NSF graduate research fellowship.

References

Bass JD (1995) Elasticity of minerals, glasses, and melts. In: Ahrens TJ (ed) Mineral physics and crystallography: a handbook of physical constants. American Geophysical Union, Washington, DC, pp 45–63

Blundy J, Wood B (1994) Prediction of crystal-melt partition coefficients from elastic moduli. Nature 372: 452–454

Boyd FR, England JL (1962) Mantle minerals. Carnegie Inst Wash Yearb 61: 107–112

Brady JB (1995) Diffusion data for silicate minerals, glasses, and liquids. In: Ahrens TJ (ed) Mineral physics and crystallography: a handbook of physical constants. American Geophysical Union, Washington, DC, pp 269–290

Burton KW, Kohn MJ, Cohen AS, O'Nions RK (1995) The relative diffusion of Pb, Nd, Sr and O in garnet. Earth Planet Sci Lett 133: 199–211

Chakraborty S, Ganguly J (1992) Cation diffusion in aluminosilicate garnets: experimental determination in spessartine–almandine diffusion couples, evaluation of effective binary diffusion coefficients, and applications. Contrib Mineral Petrol 111: 74–86

Chakraborty S, Rubie DC (1996) Mg tracer diffusion in aluminosilicate garnets at 750–850 °C, 1 atm and 1,300 °C, 8.5 GPa. Contrib Mineral Petrol 122: 406–414

Cherniak DJ (1998) Rare earth element and gallium diffusion in yttrium aluminum garnet. Phys Chem Miner 26: 156–163

Cherniak DJ, Hanchar JM, Watson EB (1997) Rare-earth diffusion in zircon. Chem Geol 134: 289–301

Coghlan RAN (1990) Studies of diffusional transport: grain boundary transport of oxygen in feldspars, strontium and the REE's in garnet, and thermal histories of granitic intrusions in south-central Maine using oxygen isotopes. PhD Thesis, Brown University, Providence

Dodson MH (1973) Closure temperature in cooling geochronological and petrological systems. Contrib Mineral Petrol 40: 259–274

Freer R, Edwards A (1999) An experimental study of Ca-(Fe, Mg) interdiffusion in silicate garnets. Contrib Mineral Petrol 134: 370–379

Frost DJ, Wood BJ (1995) Experimental measurements of the graphite C–O equilibrium and CO_2 fugacities at high temperature and pressure. Contrib Mineral Petrol 121: 303–308

Ganguly J, Tirone M (1999) Diffusion closure temperature and age of a mineral with arbitrary extent of diffusion: theoretical formulation and applications. Earth Planet Sci Lett 170: 131–140

Ganguly J, Tirone M, Hervig RL (1998) Diffusion kinetics of samarium and neodymium in garnet, and a method for determining cooling rates of rocks. Science 281: 805–807

Giletti BJ, Shanahan TM (1997) Alkali diffusion in plagioclase feldspar. Chem Geol 139: 3–20

Griffin WL, Smith D, Boyd FR, Cousens DR, Ryan CG, Sie SH, Suter F (1989) Trace-element zoning in garnets from sheared mantle xenoliths. Geochim Cosmochim Acta 53: 561–567

Harrison WJ, Wood BJ (1980) An experimental investigation of the partitioning of REE between garnet and liquid with reference to the role of defect equilibria. Contrib Mineral Petrol 72: 145–155

Jagoutz E (1988) Nd and Sr systematics in an eclogite xenolith from Tanzania: evidence for frozen mineral equilibria in continental lithosphere. Geochim Cosmochim Acta 52: 1285–1293

LaTourrette T, Wasserburg GJ (1998) Mg diffusion in anorthite: Implications for the formation of early solar system planetesimals. Earth Planet Sci Lett 158: 91–108

Mezger K, Essene EJ, Halliday AN (1992) Closure temperatures of the Sm–Nd system in metamorphic garnets. Earth Planet Sci Lett 113: 397–409

Sautter V, Harte B (1990) Diffusion gradients in an eclogite xenolith from the Roberts Victor kimberlite pipe: (2) kinetics and implications for petrogenesis. Contrib Mineral Petrol 105: 637–649

Shannon RD (1976) Revised effective ionic radii and systematic studies of interatomic distances in halides and chalcogenides. Acta Crystallogr A32: 751–767

Shimizu N (1999) Young geochemical features in cratonic peridotites from Southern Africa and Siberia. In: Fei Y, Bertka CM, Mysen BO (eds) Mantle petrology: field observations and high pressure experimentation. Geochem Soc Spec Publ 6: 47–55

Shimizu N, Pokhilenko NP, Boyd FR, Pearson DG (1999) Trace element characteristics of garnet dunites/harzburgites, host rocks for Siberian peridotitic diamonds. Proceedings of the VIIth International Kimberlite Conference, Red Roof Design. Cape Town, pp 773–782

Smith D, Boyd FR (1992) Compositional zonation in garnets in peridotite xenoliths. Contrib Mineral Petrol 112: 134–147

Smith D, Griffin WL, Ryan CG, Sie SH (1991) Trace-element zonation in garnets from The Thumb: heating and melt infiltration below the Colorado Plateau. Contrib Mineral Petrol 107: 60–79

Smyth JR, Bish DL (1988) Crystal structures and cation sites of the rock forming minerals. Allen and Unwin, Boston

Ulmer P, Luth RW (1991) The graphite–COH fluid equilibrium in P, T, f_{O_2} space. Contrib Mineral Petrol 106: 265–272

Van Orman JA, Grove TL, Shimizu N (2001) Rare earth element diffusion in diopside: influence of temperature, pressure and ionic radius, and an elastic model for diffusion in silicates. Contrib Mineral Petrol 141: 687–703

Van Westrenen W, Blundy JD, Wood BJ (1999) Crystal-chemical controls on trace element partitioning between garnet and anhydrous silicate melt. Am Mineral 84: 838–847

Wang L, Zhang Y, Essene EJ (1996) Diffusion of the hydrous component in pyrope. Am Mineral 81: 706–718

Wuensch BJ (1982) Diffusion in stoichiometric close-packed oxides. In: Bénière F, Catlow CRA (eds) Mass transport in oxides. NATO-ASI, New York, pp 353–376